Photon-induced Synthesis of Ultrafine Metal Nanoparticles on Graphene as Electrocatalyst: Impact of Functionalization and Doping

Kun Guo[a,b]*, Laura J. Rowland[a], Liam H. Isherwood[a,b], Gyorgyi Glodan[b], and Aliaksandr Baidak[a,b]

[a] *School of Chemistry, The University of Manchester, Manchester M13 9PL, United Kingdom*

[b] *Dalton Cumbrian Facility, The University of Manchester, Moor Row CA24 3HA, United Kingdom*

*Author to whom correspondence should be addressed:

K. Guo: kun.guo-2@manchester.ac.uk & kun.guo.89@gmail.com

Table of Contents

Note S1. Nucleation energy barrier and critical nucleus radius

For a spherical particle of radius r, the surface energy per unit surface area γ and the bulk free energy per unit volume of the bulk crystal ΔG_v, give a total free energy ΔG.[1, 2]

$$\Delta G = 4\pi r^2\gamma + \frac{4}{3}\pi r^3 \Delta G_v$$

The bulk free energy itself, ΔG_v is dependent on the temperature T, Boltzmann's constant k_B, the supersaturation of the solution S, and its molar volume v.

$$\Delta G_v = \frac{-k_B T ln(S)}{v}$$

Due to the surface free energy being positive and the bulk free energy being negative, it is possible to find a maximum free energy which a nucleus will pass through to form a stable nucleus by differentiating ΔG with respect to r and setting it to zero, $d\Delta G/dr = 0$, which gives a critical free energy, ΔG_c and the critical radius, r_c.

$$\Delta G_c = \frac{4}{3}\pi\gamma {r_c}^2$$

$$r_c = \frac{-2\gamma}{\Delta G_v} = \frac{2\gamma v}{k_B T ln(S)}$$

Thus, the nucleation energy barrier, ΔG_c.

$$\Delta G_c = \frac{16\pi\gamma^3 v^2}{3k_B^2 T^2 [ln(S)]^2}$$

Table S1. Average size of Pd crystalline domains of the supported composites derived by Scherrer equation from the XRD patterns.

Sample	Average size of crystalline domain[a] (nm)
Pd/GO	5.7
Pd/rGO	2.2
Pd/G	2.4
2.6-Pd/NG	2.0
1.3-Pd/NG	1.4
3.9-Pd/NG	3.8
5.2-Pd/NG	4.7

[a] calculation based on the (111) characteristic peak

Table S2. Atomic and weight percentages of C, N, O, and Pd of pristine supports and four composites from the XPS analysis.

Sample	Atomic %				Weight %			
	C	N	O	Pd	C	N	O	Pd
GO	49.26	0	50.74	0	42.15	0	57.85	0
Pd/GO	83.46	0	16.41	0.13	78.36	0	20.52	1.12
rGO	91.73	0.98	7.29	0	89.42	1.11	9.46	0
Pd/rGO	92.85	1.07	5.95	0.13	89.99	1.21	7.68	1.12
G	96.60	0	3.40	0	95.52	0	4.48	0
Pd/G	95.13	0	4.17	0.70	89.00	0	5.20	5.80
NG	89.80	5.25	4.95	0	87.60	5.97	6.43	0
Pd/NG	88.98	5.19	4.55	1.28	79.14	5.39	5.39	10.09

Table S3. Comparison of solvent, surfactant and average particle size of Pd/NG in this study and other reported metal particles prepared using high-energy radiations in the literature.

Particles	Radiation	Solvent	Surfactant	Average Size (nm)	Reference
Pd/NG	Gamma-ray	EG	–	3.0 ± 0.6	This work
Starch–Ag	Gamma-ray	H_2O	Starch	14	[3]
PVP–Ag	Gamma-ray	H_2O	Poly(vinyl pyrrolidone)	7 ± 4	[4]
PVP–Au	Gamma-ray	H_2O	Poly(vinyl pyrrolidone)	7 ± 3	[4]
PVA–Au	Electron beam	H_2O	Poly(vinyl alcohol)	50	[5]
PVA–Ag	Electron beam	H_2O	Poly(vinyl alcohol)	40	[5]
Rh–Ag	Gamma-ray	H_2O	Poly(vinyl alcohol)	15	[6]
PVP–Au	Gamma-ray	H_2O	Poly(vinyl pyrrolidone)	9.5	[7]
In	Gamma-ray	H_2O	Poly(vinyl alcohol)	12	[8]
Al–Ni	Gamma-ray	H_2O	Poly(vinyl alcohol)	4.4	[9]
PVA-Cu	Electron beam	H_2O	Poly(vinyl alcohol)	15	[10]
Ag/SiO_2	Gamma-ray	H_2O	–	15 ± 5	[11]
Au/Fe_2O_3	Electron beam	H_2O	Poly(vinyl alcohol)	3.9 ± 1.3	[12]
Pd/CNT	Gamma-ray	H_2O	Sodium dodecyl sulfate	5 ± 1	[13]
Au/Fe_2O_3	Gamma-ray	H_2O	Poly(vinyl alcohol)	5.5 ± 1.2	[14]
Ir/rGO	Gamma-ray	H_2O	Sodium dodecyl sulfate	2.3 ± 0.5	[15]
$Cu@CuAlO_2$-Al_2O_3	Gamma-ray	H_2O	Poly(vinyl pyrrolidone)	4.5	[16]

Au_1Cu_3/TiO_2	Gamma-ray	H_2O	–	6.4	[17]
Pd/Al_2O_3	Gamma-ray	H_2O	–	4.4	[18]
Au/TiO_2	Gamma-ray	H_2O	–	7	[19]
Pt_5Rh_1/C	Gamma-ray	H_2O	Tartaric acid	2.3	[20]
Pd/rGO	Gamma-ray	H_2O	–	4.7 ± 0.1	[21]
Pt/C	Gamma-ray	H_2O	Urea	2.6 ± 0.4	[22]
CoPd/CNT	Gamma-ray	H_2O	–	15	[23]
PtRu/CNT	Gamma-ray	H_2O	Vinyl pyrrolidone	11	[24]

Table S4. Binding energies of pyridinic, pyrrolic and graphitic N of pristine NG and four Pd/NG composites from the XPS analysis.

Sample	Binding energy (eV)		
	Pyridinic N	**Pyrrolic N**	**Graphitic N**
NG	398.2	400.4	402.7
1.3-Pd/NG	398.1	400.0	401.9
2.6-Pd/NG	398.1	400.0	401.7
3.9-Pd/NG	398.0	399.7	401.5
5.2-Pd/NG	398.0	399.7	401.4

Table S5. Atomic and weight percentages of C, N, O, and Pd of pristine NG and four Pd/NG composites from the XPS analysis.

Sample	Atomic %				Weight %			
	C	N	O	Pd	C	N	O	Pd
NG	89.80	5.25	4.95	0	87.60	5.97	6.43	0
1.3-Pd/NG	90.49	5.34	3.45	0.72	84.00	5.78	4.27	5.96
2.6-Pd/NG	88.98	5.19	4.55	1.28	79.14	5.39	5.39	10.09
3.9-Pd/NG	87.97	5.25	5.07	1.71	75.81	5.28	5.82	13.09
5.2-Pd/NG	87.40	4.83	5.66	2.11	73.29	4.72	6.32	15.66

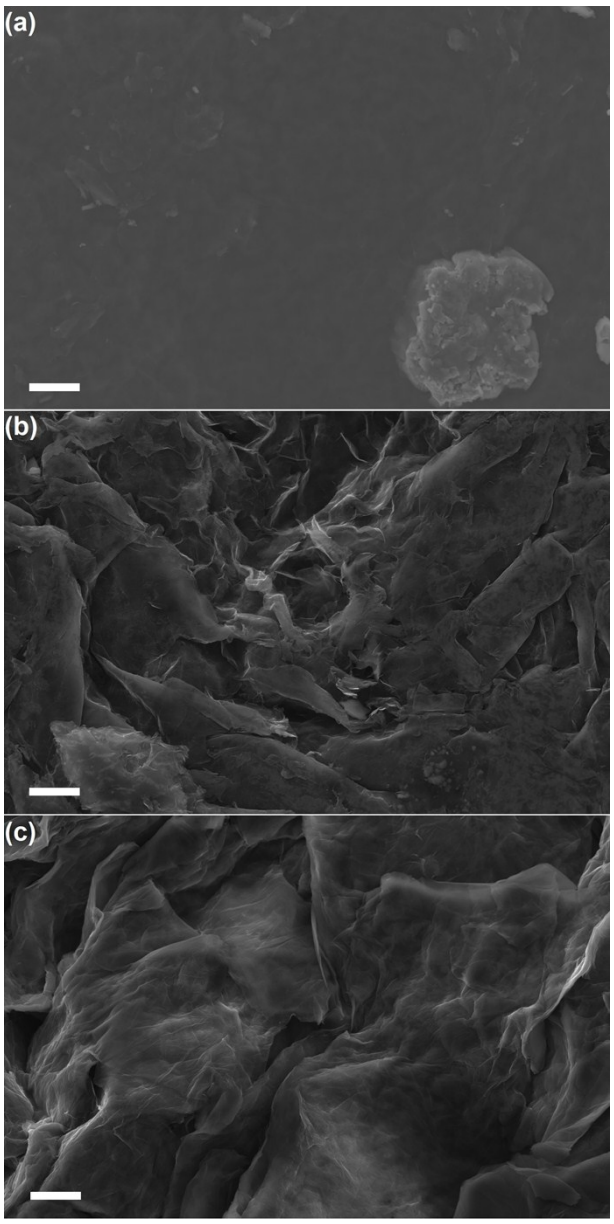

Figure S1. Representative SEM images of pristine GO (a) and GO irradiated in H_2O (b) and EG (c). Scale bar: 5 μm.

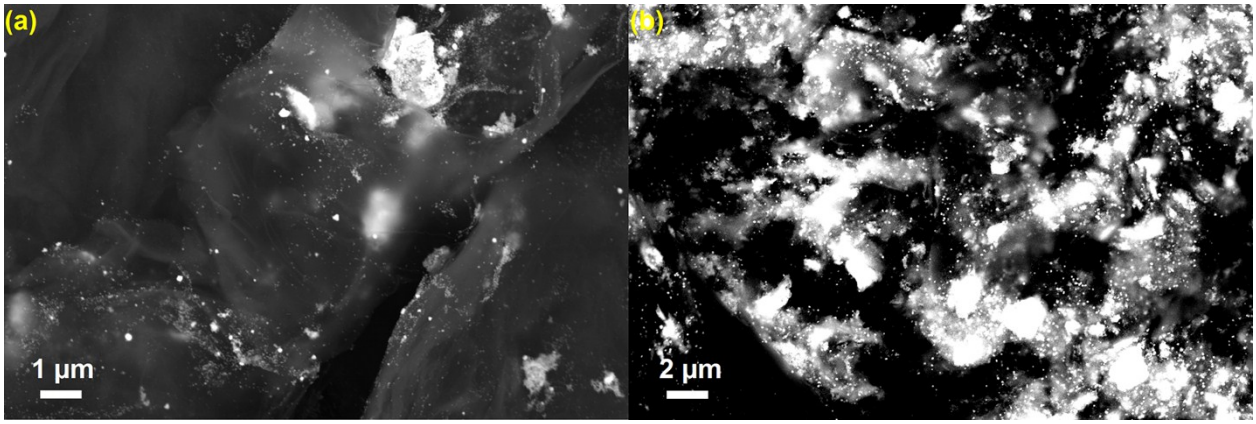

Figure S2. Representative SEM images of 1 mM Pd/GO (a) and 2 mM Pd/GO (b) after gamma irradiation in EG.

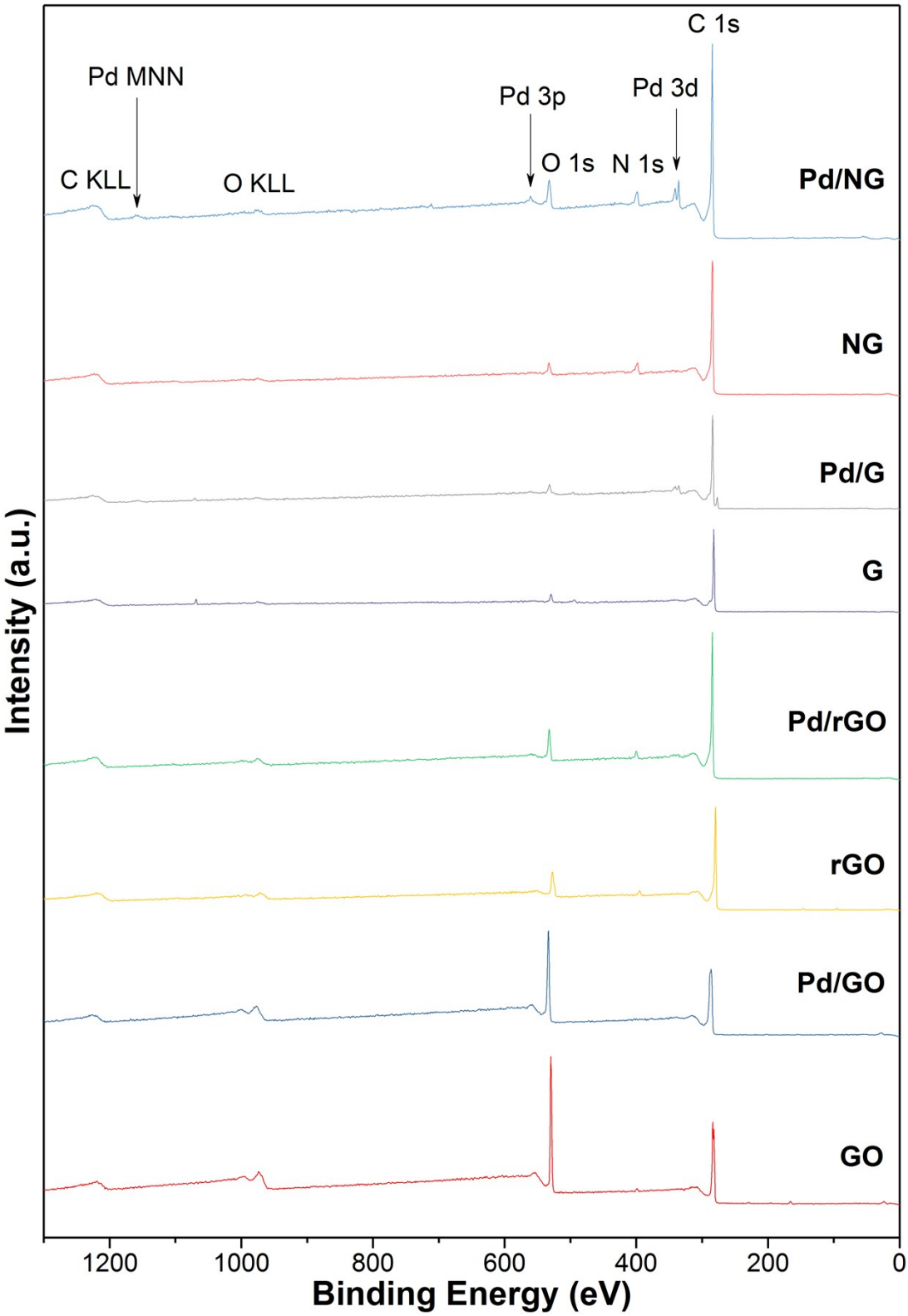

Figure S3. Full survey XPS spectra of pristine supports and supported composites.

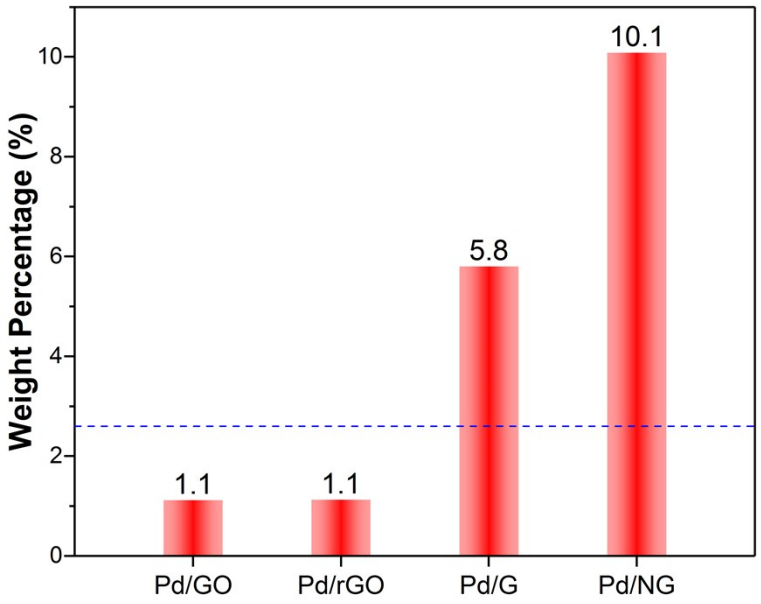

Figure S4. Pd loading in weight percentage of four supported composites. The blue horizontal line indicates the nominal loading of 2.6 wt %.

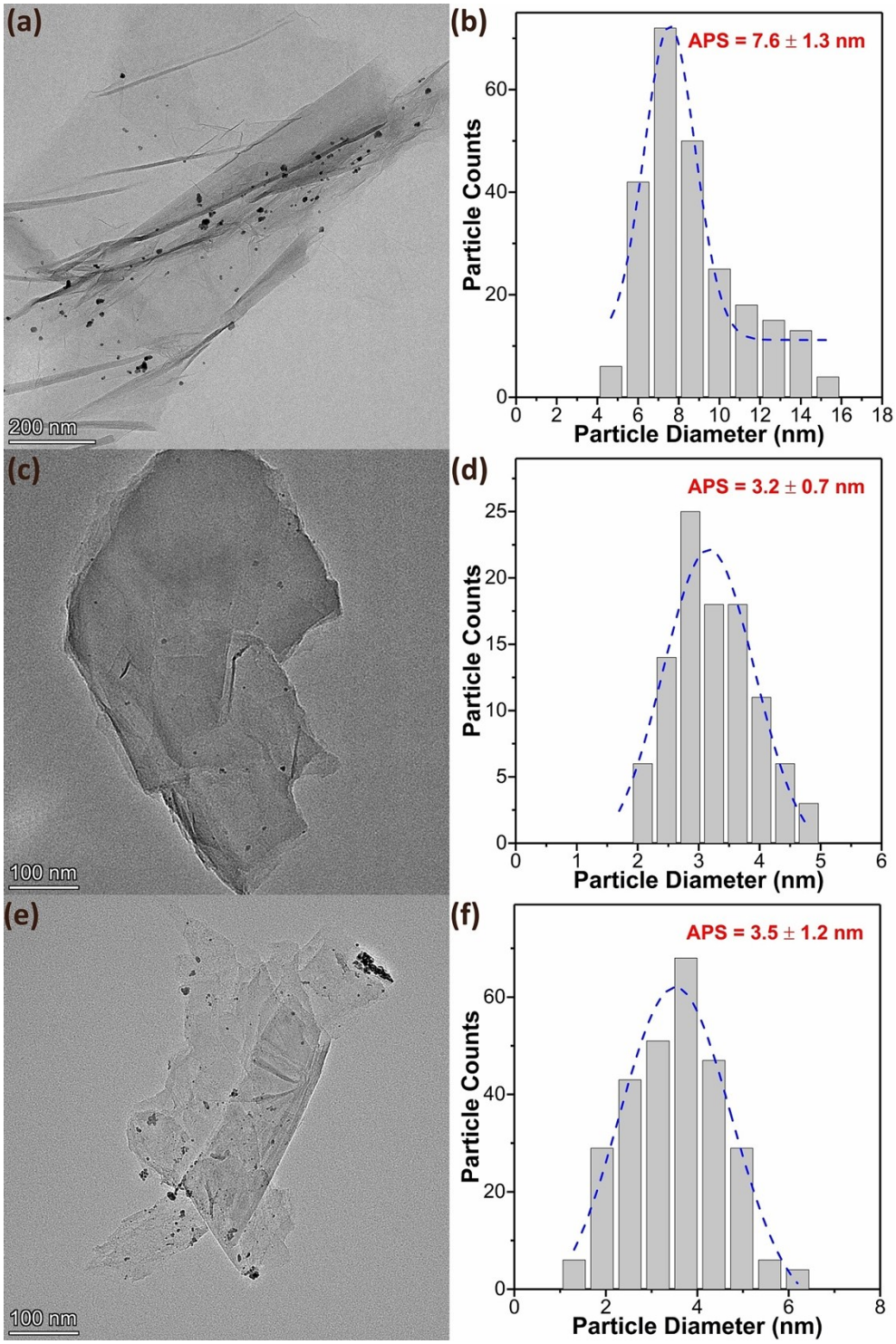

Figure S5. Representative TEM images and corresponding PSDs of the composites: Pd/GO (a, b), Pd/rGO (c, d) and Pd/G (e, f).

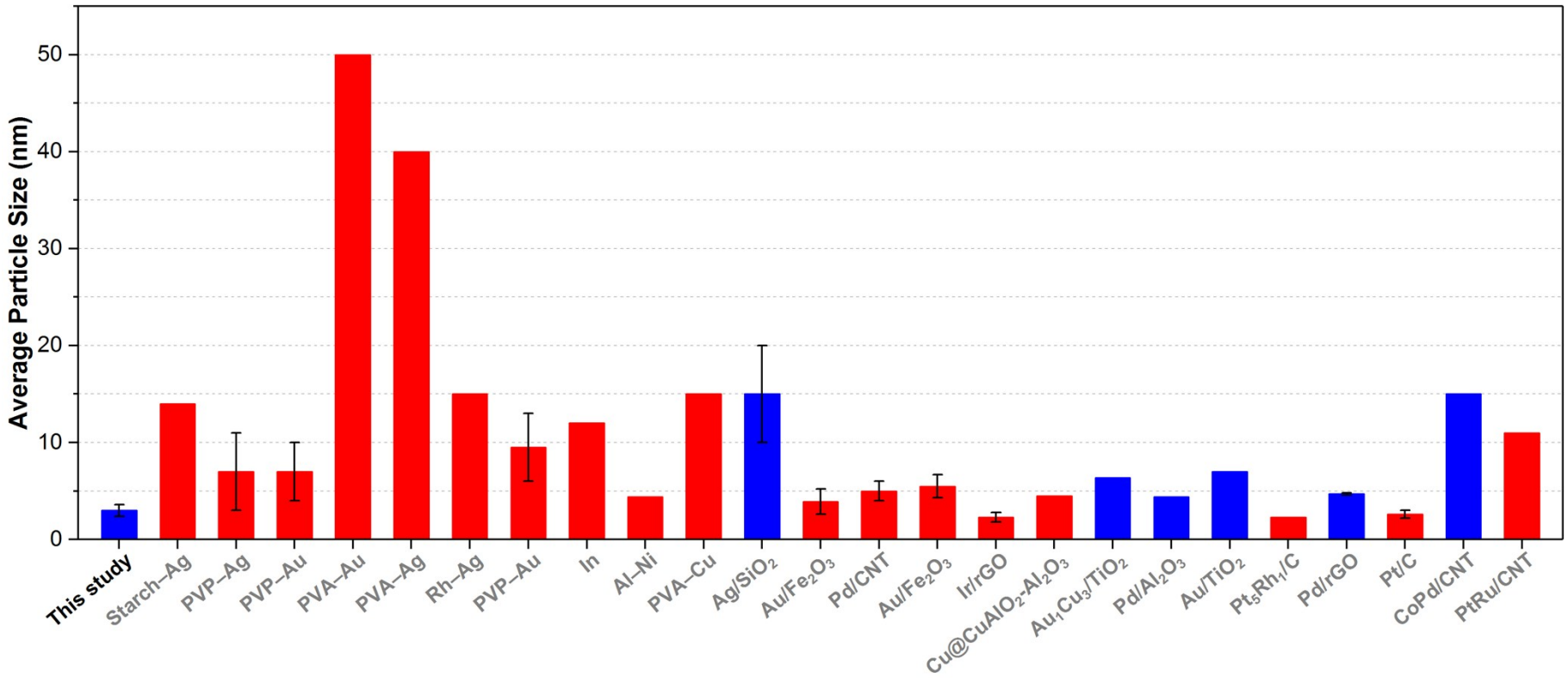

Figure S6. Comparison of average particle size of Pd/NG in this study and reported metal particles prepared by high-energy radiation in the literature. Blue bars refer to the absence of surfactants and red bars refer to the presence of surfactants in the synthesis.

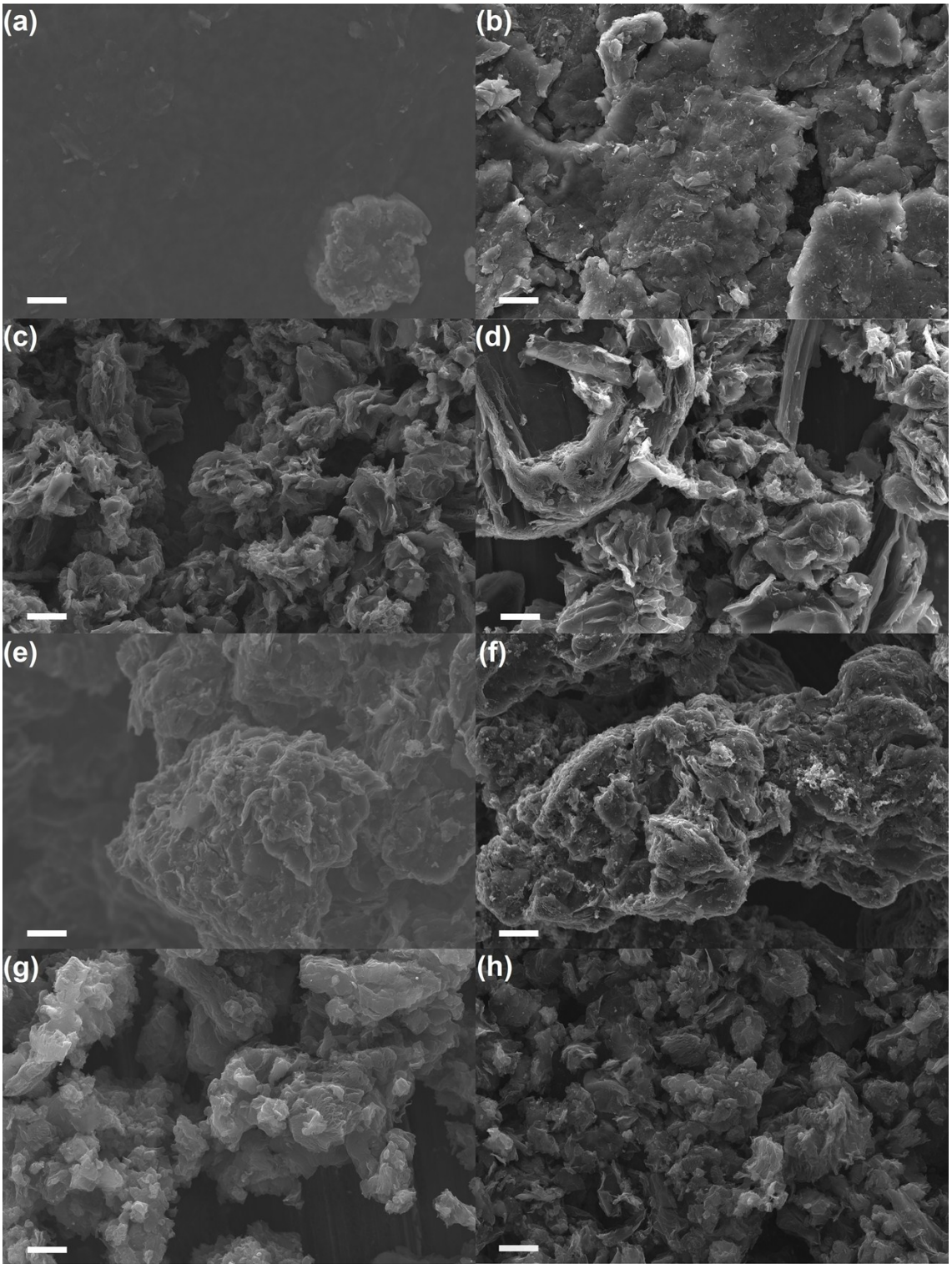

Figure S7. Representative SEM images of pristine supports and supported composites: GO (a) and Pd/GO (b), rGO (c) and Pd/rGO (d), G (e) and Pd/G (f), and NG (g) and Pd/NG (h). Scale bar: 5 μm.

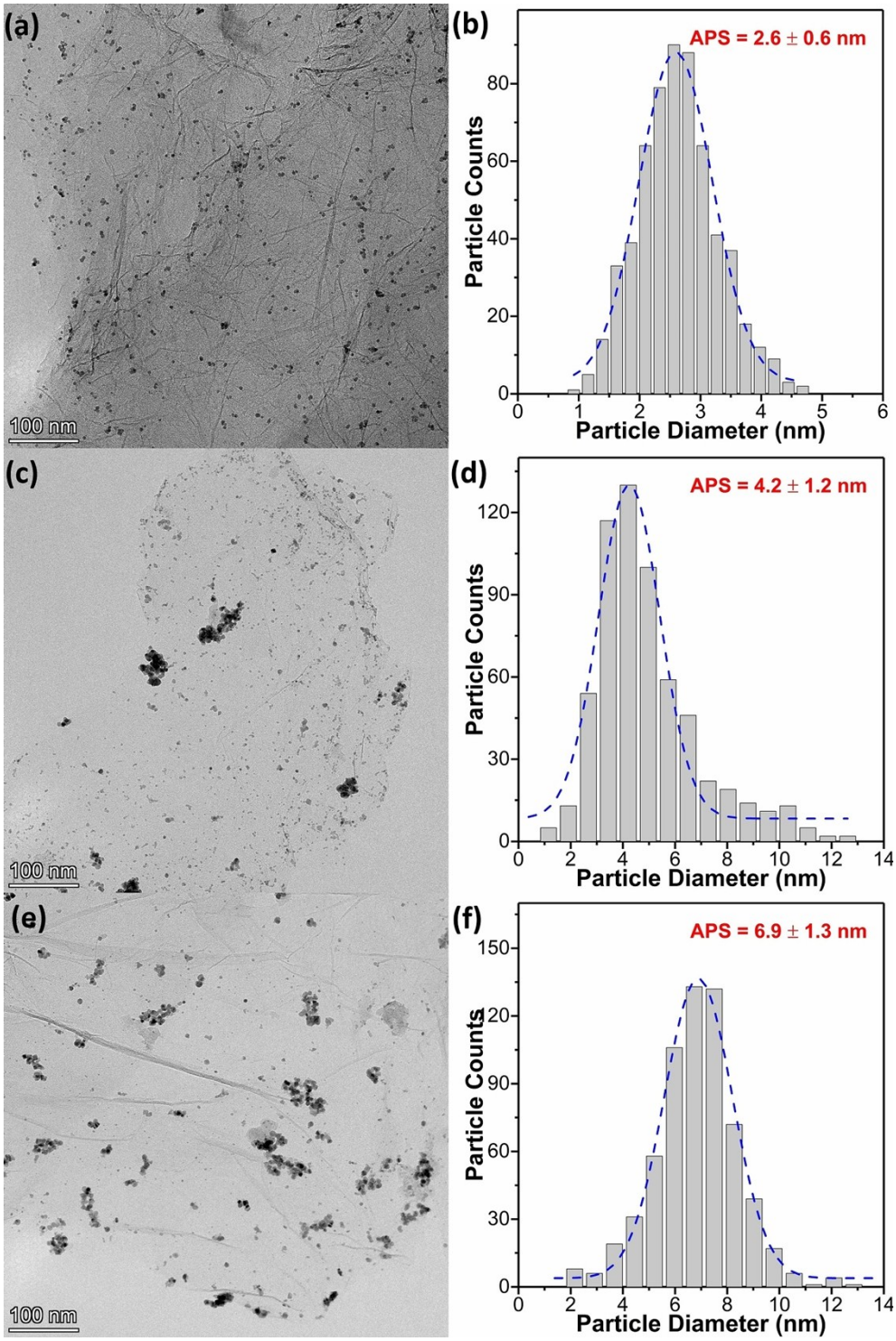

Figure S8. Representative TEM images and corresponding PSDs of the Pd/NG composites: 1.3-Pd/NG (a, b), 3.9-Pd/NG (c, d) and 5.2-Pd/NG (e, f).

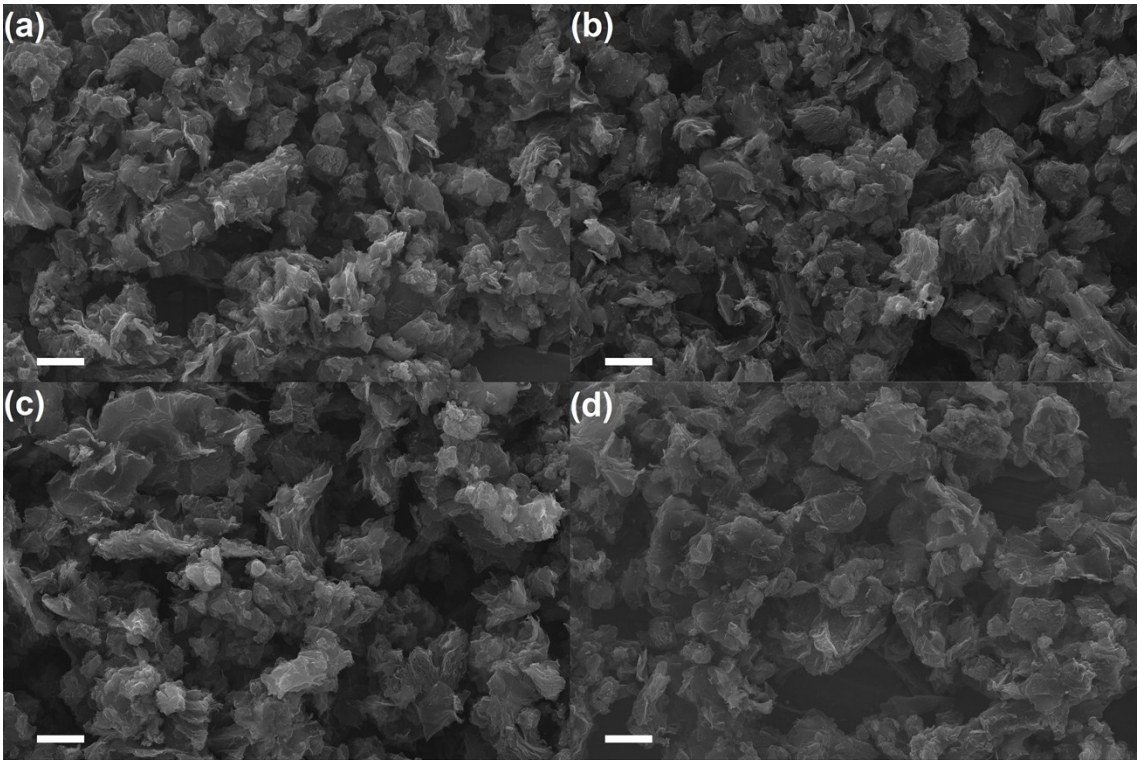

Figure S9. Representative SEM images of four Pd/NG composites: 1.3-Pd/NG (a), 2.6-Pd/NG (b), 3.9-Pd/NG (c), and 5.2-Pd/NG (d). Scale bar: 5 μm.

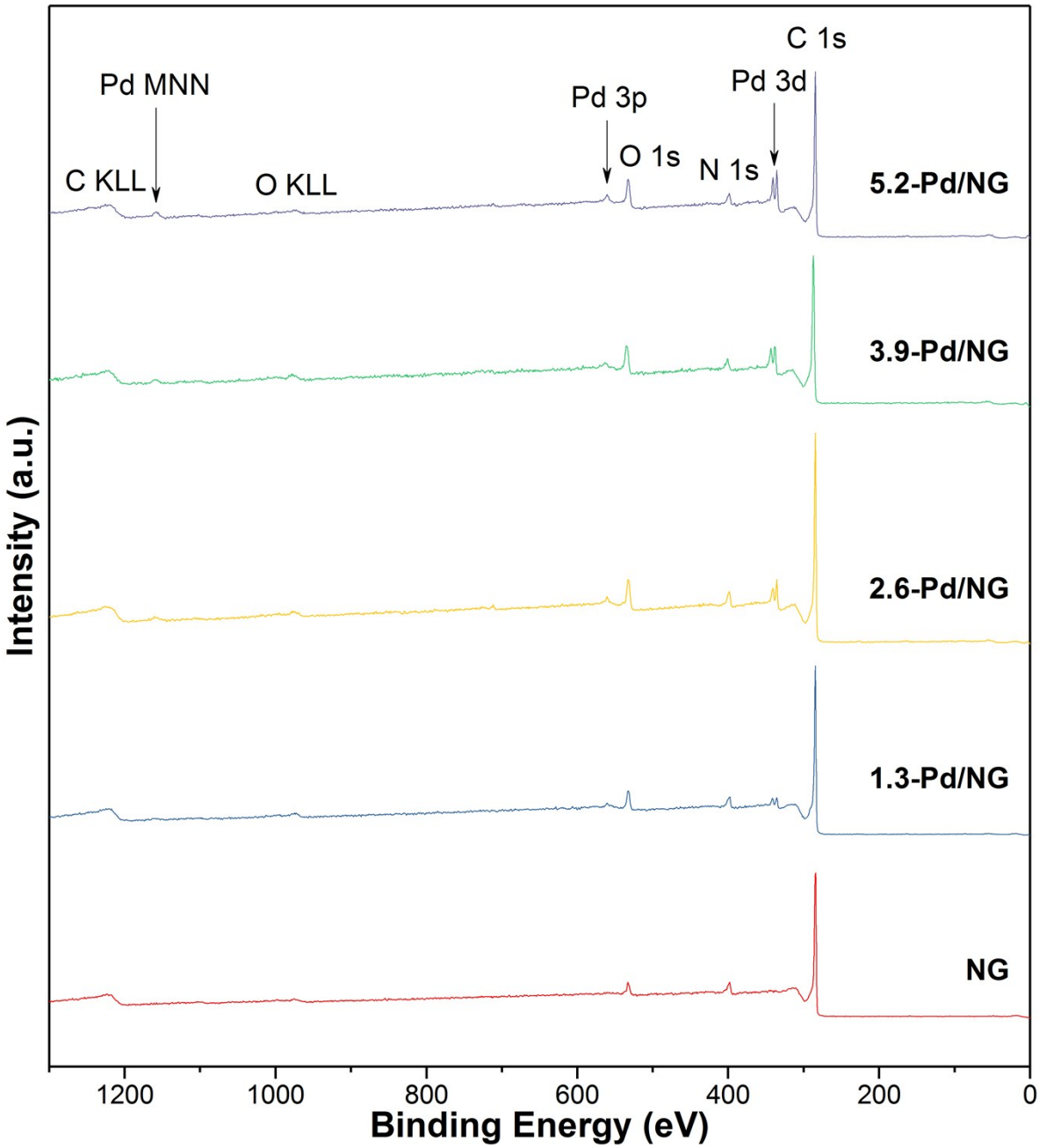

Figure S10. Full survey XPS spectra of pristine NG and Pd/NG with different Pd loadings.

References

1. N. T. Thanh, N. Maclean and S. Mahiddine, *Chem. Rev.*, 2014, **114**, 7610–7630.
2. K. Huang, L. Zhang, T. Xu, H. Wei, R. Zhang, X. Zhang, B. Ge, M. Lei, J. Y. Ma, L. M. Liu and H. Wu, *Nat. Commun.*, 2019, **10**, 606.
3. M. Z. Kassaee, A. Akhavan, N. Sheikh and R. Beteshobabrud, *Radiat. Phys. Chem.*, 2008, **77**, 1074–1078.
4. T. Li, H. G. Park and S.-H. Choi, *Mater. Chem. Phys.*, 2007, **105**, 325–330.
5. S. K. Mahapatra, K. A. Bogle, S. D. Dhole and V. N. Bhoraskar, *Nanotechnology*, 2007, **18**, 135602.
6. K. Torigoe, H. Remita, P. Beaunier and J. Belloni, *Radiat. Phys. Chem.*, 2002, **64**, 215–222.
7. N. Misra, J. Biswal, A. Gupta, J. K. Sainis and S. Sabharwal, *Radiat. Phys. Chem.*, 2012, **81**, 195–200.
8. Y. Liu, Y. Qian, M. Zhang, Z. Chen and C. Wang, *Mater. Lett.*, 1996, **26**, 81–83.
9. A. Abedini, F. Larki, E. Saion, A. Zakaria and M. Z. Hussein, *Radiat. Phys. Chem.*, 2012, **81**, 1653–1658.
10. F. Zhou, R. Zhou, X. Hao, X. Wu, W. Rao, Y. Chen and D. Gao, *Radiat. Phys. Chem.*, 2008, **77**, 169–173.
11. S. P. Ramnani, J. Biswal and S. Sabharwal, *Radiat. Phys. Chem.*, 2007, **76**, 1290–1294.
12. S. Seino, T. Kinoshita, T. Nakagawa, T. Kojima, R. Taniguci, S. Okuda and T. A. Yamamoto, *J. Nanopart. Res.*, 2007, **10**, 1071–1076.
13. J. V. Rojas and C. H. Castano, *Radiat. Phys. Chem.*, 2012, **81**, 16–21.
14. S. Seino, T. Kinoshita, Y. Otome, T. Maki, T. Nakagawa, K. Okitsu, Y. Mizukoshi, T. Nakayama, T. Sekino, K. Niihara and T. A. Yamamoto, *Scr. Mater.*, 2004, **51**, 467–472.
15. J. V. Rojas, M. C. Molina Higgins, M. Toro Gonzalez and C. E. Castano, *Appl. Surf. Sci.*, 2015, **357**, 2087–2093.
16. A. Abedini, E. Saion, F. Larki, A. Zakaria, M. Noroozi and N. Soltani, *International Journal of Molecular Sciences*, 2012, **13**, 11941–11953.
17. Z. Hai, N. El Kolli, J. Chen and H. Remita, *New Journal of Chemistry*, 2014, **38**, 5279–5286.
18. H. Yu, Z. Mao, W. Dai, J. Peng, M. Zhai and G. Wei, *Appl. Catal. A: Gen.*, 2012, **445–446**, 246–251.
19. A. Lafon, M. Tréguer-Delapierre, D. Bazin and C. Faure, *Colloid Polym. Sci.*, 2012, **290**, 1015–1022.
20. Y. Matsuura, S. Seino, T. Okazaki, T. Akita, T. Nakagawa and T. A. Yamamoto, *Radiat. Phys. Chem.*, 2016, **122**, 9–14.
21. S. Ghosh, Y. Holade, H. Remita, K. Servat, P. Beaunier, A. Hagège, K. B. Kokoh and T. W. Napporn, *Electrochim. Acta*, 2016, **212**, 864–875.
22. H.-Y. Park, D.-S. Yang, D. Bhattacharjya, M. Y. Song and J.-S. Yu, *Int. J. Hydrog. Energy*, 2014, **39**, 1688–1697.
23. K.-P. Lee, S.-H. Lee, K. Shanmuga Sundaram and G. Anantha Iyengar, *Radiat. Phys. Chem.*, 2012, **81**, 1422–1425.
24. S.-Y. Kwon, H.-D. Kwen and S.-H. Choi, *J. Sens.*, 2012, **2012**, 1–8.